Al Implantation in SiC; Where Will the Ions Come to Rest?

Margareta K. Linnarsson[1,a], Lasse Vines[2,b] and Anders Hallén[3,c] *

[1]Department of Physics and Astronomy, Uppsala University, P.O. Box 516, SE 751 20, Sweden

[2]Physics Department/Center for Materials Science and Nanotechnology, University of Oslo, P.O. Box 1048 Blindern, N-0316 Oslo, Norway

[3]KTH Royal Institute of Technology, School of EECS, Electrum 229, SE-164 40 Kista, Sweden

[a]margareta.linnarsson@physics.uu.se, [b]lasse.vines@fys.uio.no, [c]ahallen@kth.se

*corresponding author

Abstract. In all implantations into crystalline targets, quite a few ions find a path along a crystal channel or plane, so called channeling, and these ions travel deep into the crystal. This paper treats aluminum (Al) implantation in 4H-SiC and show how the crystal lattice will guide incoming ions deep into the target and modify the final dopant distribution. 4H-SiC samples have been implanted with 100 keV Al-ions, in a "random" direction using the wafer miscut angle of 4°, as well as with the impact beam aligned anti-parallel to the [0001] direction. Aluminium concentration versus depth profiles has been recorded by secondary ion mass spectrometry (SIMS). To track the most probable ion paths during stopping process, SIIMPL, a Monte Carlo simulation code based on the binary collision approximation (MC-BCA) has been used. In addition, the remaining ion energy has been extracted from SIIMPL at various depth along the ion path. Our results show that, independent of the used impact angle, some ions will be steered by crystal planes predominantly into the $[000\bar{1}]$ direction and also along the six $< 11\bar{2}3 >$ directions. The energy loss is smaller along these low index axes. Therefore, at a depth of 1.2 μm, some Al ions along a $< 11\bar{2}3 >$ path may still have kinetic energy, more than 40% of the original 100 keV, and continues to move deep into the SiC sample. The mean projected range of 100 keV ions in 4H-SiC is about 120 nm.

Introduction

To introduce dopants in semiconductors, ion implantation is a useful tool [1, 2]. Single crystalline semiconductors are commonly used for device fabrication, which means that the crystal structure with open channels and planes can play an important role to determine the final position of the implanted ion [3-5]. For implantations in 4H-SiC wafers, the four degrees standard miscut is usually employed as a "random", non-channeling direction. This approach is expected to result in a slightly skewed Gaussian depth profile, i.e. a well-defined depth distribution of the dopant atoms determined by the dose and the used ion energy. When performing implantations in a "random" direction, it is often assumed that the ions do not follow a path along low index crystal directions, although it has been shown that already after a few collisions with target atoms, the incoming ions have changed direction and may find a crystal direction where they can be steered deep into the crystal [6-9]. On the other hand, if the implantation is deliberately performed along a low index crystal axis, many ions will move substantially deeper into the SiC crystal [10]. This extended range of channeled ions is usually seen as a broadening of the implanted profiles to larger depths and can even be used to obtain deep box-shaped structures. Besides from the angle of incidence, the probability for an ion to be channeled, or de-channeled, in 4H-SiC is also strongly affected by damage in the lattice and implantation temperature [11, 12].

In this study, we have investigated the probability for intentional and unintentional channeling during Al implantation in 4H-SiC. The study combines experimental data and simulations to track the most likely ion path in the crystal with a special focus on "unexpected" deep ion paths as a result of channeling.

Experimental

An epitaxial structure with a 10 μm thick, n-type epitaxial layer (5×10^{15} N/cm^3) grown on a 4° miscut 4H-SiC substrate has been used. Two varieties of 100 keV aluminum implantations have been performed along the [000$\bar{1}$] direction: at room temperature (RT) and at 600 °C. A third implantation was also performed at RT in a "random" direction, taking advantage of miscut of the sample, i.e., at 4° off from the $< 0001 >$ direction towards $< 11\bar{2}0 >$ direction.

Before the implantation, the crystal orientation relative to the incoming beam has been deduced. For this, a 100 keV proton beam has been used to acquire the blocking pattern, "channel maps", for the backscattered protons using a medium ion energy spectrometer (MEIS) with a high-precision, six-axis goniometer and a large area, ϕ120 mm, position sensitive detector [13].

After alignment of the sample, the ion source was reconfigured and Al implantations where performed. The resulting depth distributions of Al was determined by secondary ion mass spectrometry (SIMS) in a Cameca IMS7f micro analyzer. A primary sputtering beam of 10 keV $^{32}(O_2)^+$ ions was applied and positive secondary ions were detected.

Simulations

The simulations have been performed to predict preferential ion paths and study the role of the crystal structure to guide the ions deep into the sample. The Monte-Carlo binary collision approximation (MC-BCA) code SIIMPL, developed in-house, has been employed [14]. In this code, the universal potential of Ziegler, Biersack and Littmark (ZBL) [15] has been used and the scattering integral has been solved by the "Magic- Formula" [16]. The lower electronic stopping in channels has been accounted for by modifying the random electronic loss, S_e, by the expression $S_e A exp(-sp/a_u)$, where s, p, a_u and A are: a fitting constant, the impact parameter, the universal screening length and a normalization constant, respectively. The random electronic stopping, S_e, is expressed as kE^b where k and b values of 4.0 and 0.515, respectively, has been utilized for Al-ions [17]. Thermal vibrations have been included in the model according to the mean-square displacement of carbon and silicon atoms at RT, 0.057 and 0.051 Å, respectively [18], while at 600 °C the mean-square displacements have been determined to 0.091 and 0.082 Å by fitting simulations with experimental data for different ions and doses [6]. Dynamic annealing of damage has also been included in the model [19]. The native self-oxide and adhesive contaminations at the surface are approximated by an amorphous top-layer of 8 and 4 Å at RT and 600 °C, respectively [6].

In addition, SRIM [20] calculations have been performed. In these calculations the atomic density of crystalline 4H-SiC has been used. The SRIM algorithms treats the sample as amorphous.

Result and Discussion

Figure 1 shows, a typical blocking pattern for 100 keV protons for a 4H-SiC crystal, where backscattered ions are recorded by a 2D-detector. The x- and y-scales relates to the detector size. Darker areas represent lower backscatter yield and corresponds to low index crystal directions and planes in the crystal. The $< 0001 >$ direction in the crystal is easily identified from the six-fold symmetry, i.e., the point where the $\{1\bar{1}00\}$ and the $\{11\bar{2}0\}$ planes, in total six lines, cross each other. If the sample and the detector is placed in parallel, the off angle of the sample, the miscut, will place the <0001> direction off from the detector center, marked in the figure by a white dot. This kind of measurements has been used as a tool to identify different crystal directions and align the incoming beam in relation to the requested sample direction before ion implantation.
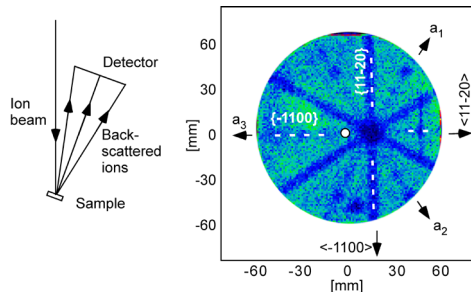
Fig. 1. Protons backscattered from a 4H-SiC sample recorded by a 2D-detector, used for aligning the crystal before implantation. Here, the sample is placed in parallell to the detectore, i.e., the surface normal are close to the center of the detector and the sample miscut of 4° is easily recognized.
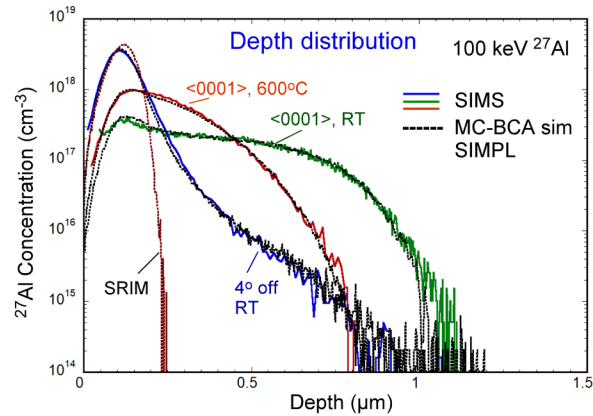
Fig. 2. SIMS measurements of Al concentration versus depth for three,100 keV implantations. One implantation is done in non-channeling direction at RT (blue) and two implantations are made along [000$\bar{1}$] direction at RT (green) and 600° C (red), respectively. In addition, MC-BCA simulations with the SIIMPL [14] code and SRIM [20] simulations are also included (dotted).

The three different 100 keV Al implantations at a fluence in the 10^{13} cm^{-2} range, as recorded by SIMS, are displayed in Fig. 2 Two implantations are made at RT, one along the [000$\bar{1}$] direction and one anti-parallel to the surface normal, 4° off from $< 0001 >$, a commonly used direction taking advantage of the miscut of the sample to obtain a non-channeling direction. The third implantation is made at 600 °C along the crystal direction [000$\bar{1}$]. The non-channeling implantation results in a skewed Gaussian profile with a long tail on the deep side, while the channeled implantations at RT are more box-shaped and substantially deeper than the predicted depth of the implanted ions according to SRIM (see Fig. 2). The SRIM simulation shows the expected profile for an amorphous target of the same density as the crystalline 4H-SiC target. If the sample temperature is increased during channeled implantation, the de-channeling increases and the profile does not extend as deep as in the RT case, as shown by the red curve in Fig. 2. The projected range, roughly equal to the peak position, is similar to the implantation in non-channeling direction, but as expected, the long deep tail, down to 1 μm, is not present. However, excellent fits of measured data are obtained with MC-BCA simulations using the SIIMPL code, included in Fig.2 as black dotted lines. In SIIMPL the crystal structure is taken into account. To further investigate the nature of the deep tails, the ion direction and energy at several depths has been extracted from the SIIMPL simulations.

In a MC-BCA simulation with SIIMPL, a random number is used to select the start position where an ion hits the oxidized/amorphous sample surface, after which the ion path is calculated for each collision with target atoms according to BCA theory. This is repeated for a large number of incoming ions and from such a simulation, the probability that an ion follows some preferential directions at particular depth can be extracted. As an example, this is shown in Fig. 3, where the studied depth is indicated in a SIMS profile with an orange dotted line in Fig. 3a, while Fig. 3b illustrates that an incoming ion changes direction many times, as it travels deeper into the crystal. In Fig. 3c the ion distribution has been extracted at a depth of 0.6 μm and plotted as a 3D surface and also projected on a 2D surface, similar to the detector in a transmission experiment. On the average, the distance between two collisions in 4H-SiC in this energy range and at room temperature is 1.3 Å. An ion, reaching a depth of 0.6 μm, has therefore been deflected thousands of times and the target atoms may have steered the ions into some preferential directions, i.e. low index crystal directions.
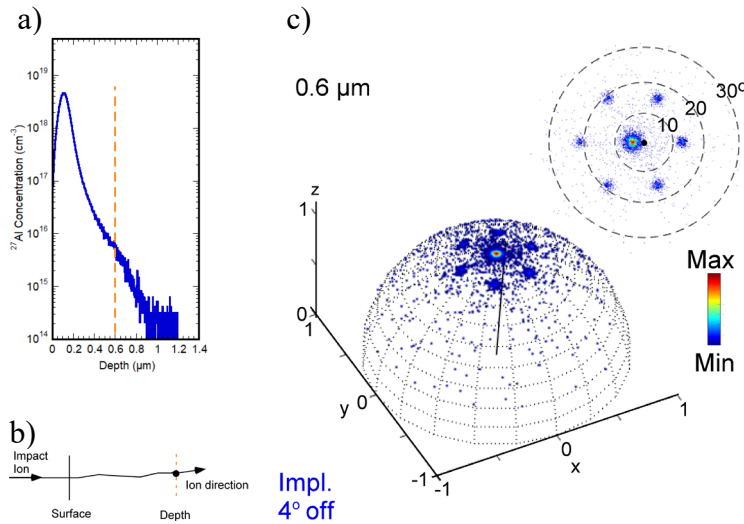
a)

c)

Fig. 3. In a) the Al concentration versus depth is shown and the depth of 0.6 μm is indicated by an orange, dotted line. b) As an ion travel into a crystal, it collides with target atoms, change direction and loses energy. c) The preferable direction of the ions at a depth of 0.6 μm are drawn on a half-sphere and on a plane perpendicular to the impact direction. The black line from [0 0 0] to [0 0 1] in the half-sphere and black dot at [0 0] in the planar view shows the direction of the incoming ion. In the planar view, three dotted circles indicate angular distance of 10°, 20° and 30° from the center.

The probability for a particular direction at this depth is given by multi-color scale where red and blue colors stand for high and low intensity, respectively. A pattern with a larger central spot surrounded by six smaller dots is visible in the figures indicating seven preferred directions for the incoming ions that have reached this depth. A black line and a black dot in the half-sphere and the planar view, respectively, indicates the original direction of the incoming ion. The three concentric circles in the 2D view is drawn at directions representing angles of 10°, 20° and 30° from the incident direction. The main probability to find an ion, the central spot, is displaced by 4° from the original ion direction. This is caused by the miscut of the sample, used for implantation in a non-channeling direction. At the depth of 0.6 μm, after a large number of collisions, the ions have been guided by the target atoms into the $[000\bar{1}]$ channel and at this depth, the $[000\bar{1}]$ direction is preferred. However, some ions may also follow $< 11\bar{2}3 >$ directions, resulting in six-fold symmetry, shown as six dots at 17° from the $[000\bar{1}]$ direction. The same kind of simulations has been made at several depths between 25 Å and 1.2 μm for the implantations 4° off from $[000\bar{1}]$ and these are displayed in Fig.4.

In Fig. 4, starting from the surface, at a depth of 25 Å, (a) ions are mainly following the original impact direction, giving the highest probability in the center of the image, seen as a small lighter colored spot. A slightly higher intensity is also revealed along 6 planes in the crystal forming a "star-like" image extending the ion distribution to larger angels, while the probability for the major part of the ions to be scattered more than 20° (the second circular ring) from the original direction is still small. After about 40 interactions with target atoms, at a depth of 5 nm, it is clearly evident that the ions are steered by the crystal planes and also avoids certain directions. The ions close to the middle form eventually, for larger depths, a hexagonal ring, originating from the six-fold symmetry of 4H-SiC crystals. For the shallower depths, two directions are the most likely ones, where two planes cross on the right-hand side. The hexagonal ring is centered around the $[000\bar{1}]$ direction. As the depth increases, the intensity on the side closer to the impact direction decreases and the diameter of the ring closes in on the $[000\bar{1}]$ direction. Also, a star-like pattern from the six crossing planes, is revealed at 0.1 μm from the surface (f). The following figure (g) is from 0.2 μm. At this point, the main part of the Al-ions is following $[000\bar{1}]$ direction but the six $< 11\bar{2}3 >$ directions, as well as a few more directions are present, visible as dots, farther out, at higher angles. In addition to channeling along low index direction, planar channeling may occur along $\{11\bar{2}0\}$ planes. The star-like pattern is close to symmetric and displaced 4° from the surface normal and the original direction has no longer any major influence on the most likely track.
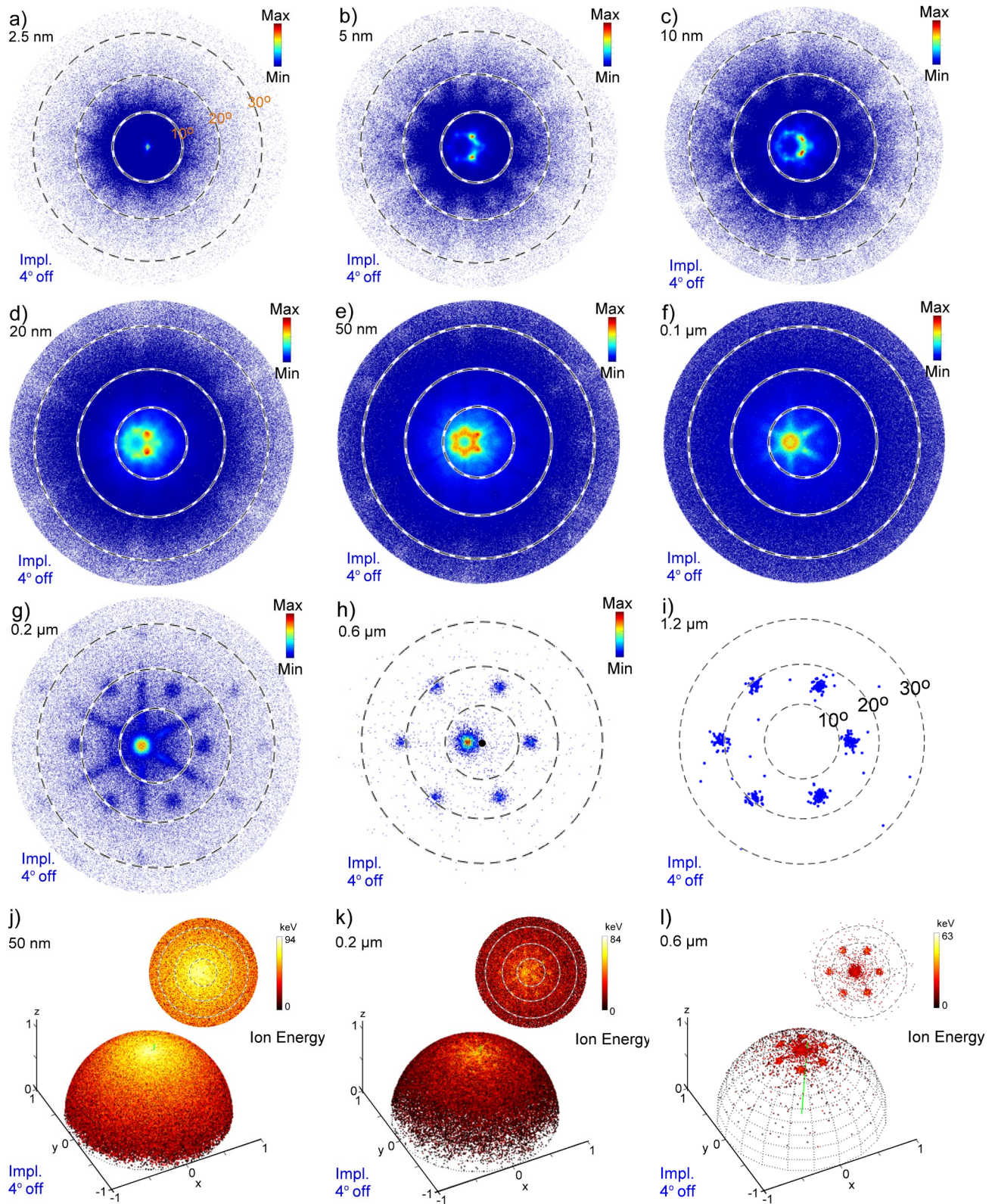
Fig. 4. Simulation of preferential directions and remaining energy of Al-ions during implantation in 4H-SiC at various sample depths. Preferential directions are displayed at 2.5 nm to 1.2 μm (a-i), and remaining ion energy at 50 nm to 0.6 μm (j-l). 100 keV Al-ions has been implanted parallel to the surface normal, using the miscut angle of 4°. The angle from the impact direction has been indicated at 10, 20 and 30° by white and black, dotted circles. The impact direction has been indicated by a black dot in (h) and a green line in (j), (k) and (l). The SIIMPL code has been used in the simulations [14].

In the tail, at 0.6 µm (h), a few ions will still move along the $[000\bar{1}]$ and, with lower probability, along the six $< 11\bar{2}3 >$ axial directions. Planar channeled ions have stopped before this point and no lines related to low index planes are observed in the image. Further down (i), only ions that have followed $< 11\bar{2}3 >$ directions will "survive". This may be expected, as it is known that channel implantations along the $< 11\bar{2}3 >$ direction compared to the $[000\bar{1}]$ direction will result in a deeper Al profile [10, 18]. Note that planar channeling cannot be excluded in the final distribution of the ions and it is particular important closer to the surface.

One more property of the ions, other than their direction, that can be extracted from the simulations is their energy along the path, which determines the final position where the ion will come to rest. The remaining energy of the moving ions at three depths is displayed in Fig. 4, j-l. At 50 nm from the surface (j), the energy loss decreases as the angle increases and no pronounced pattern related to the crystal is present, but a small mismatch of the maximum remaining energy according to the miscut of the sample. A green line in the half-sphere in Fig. 4j marks the original impact direction. However, at 0.2 µm (k), a pattern is visible with lower energy loss along low index direction and planes. A crossing of three $\{11\bar{2}0\}$ planes indicates ions of higher energy and, also, a lighter dot in the $[000\bar{1}]$ direction can be easily distinguished. In these directions, the channeled Al ions have lost less than 20% of their energy. In the final panel, at 0.6 µm (l), the ions travel along axial channels and have preserved more than half of the original energy and, therefore, may travel very far particularly along the $< 11\bar{2}3 >$ directions before coming to rest.

Figure 5 shows preferential ion directions and remaining energy for channeled implantations with 100 keV Al-ions along the $[000\bar{1}]$ direction. At depths of 0.6 µm (Fig .5 a and e), most of the ions will move along the $[000\bar{1}]$ direction but, in addition, the main track is surrounded by six dots, $< 11\bar{2}3 >$ directions. Before the depth of 1.2 µm (Fig.5 c and h), Al-ions moving along the $[000\bar{1}]$ direction have lost their energy and come to rest while Al-ions along a $< 11\bar{2}3 >$ track are still mobile although the probability to be scattered into these directions is low. Comparing the three implantations in Fig. 4 h and Fig. 5 a and e, at a depth of 0.6 µm, the most energetic ions at this depth will follow the $[000\bar{1}]$ direction, while the probability for an ion to be scattered into a $< 11\bar{2}3 >$ direction is smaller in the aligned implantation
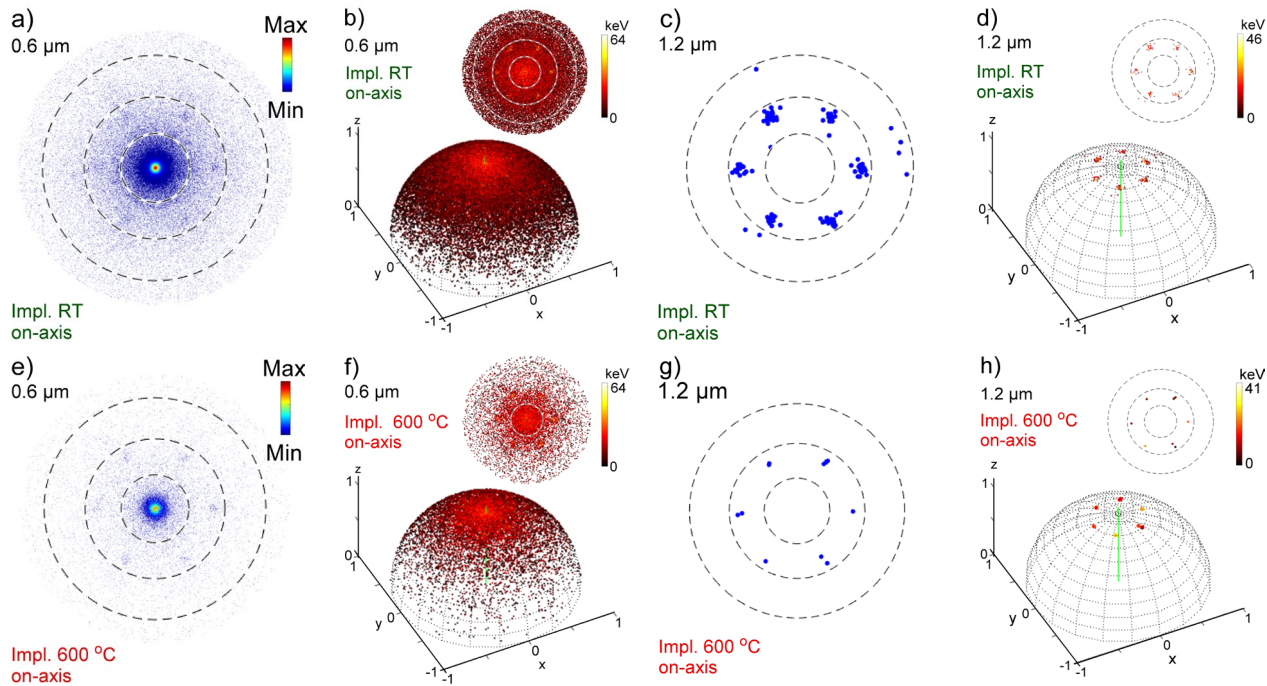

Fig. 5. Simulation of the probability to find an Al-ion moving in a particular direction at a depth of 0.6 µm (a and e) and 1.2 µm (c and h) during Al implantation along the $[000\bar{1}]$ direction, on-axis, at RT (a and c) and 600 °C (e and h). The remaining energies in keV is given in b, d, f and g for the pseudo ions in a, c, e and g, respectively. SIIMPL is used for the simulations [14].

The maximum remaining energy of some Al-ions in Fig. 4 l and Fig. 5 b and f are similar independent of impact direction and temperature, but the probability to find an ion at this depth varies with the used implantation geometry and temperature. For example, if an ion follows a track along a $< 11\bar{2}\bar{3} >$ direction, it still carries more than 40 keV at a depth of 1.2 μm, Fig. 5 d and h. This means that open, low index, directions in a crystal targets facilitates for ions to move far into the sample during implantation. Even though the concentration of channeled ions is relatively low, as seen in SIMS depth profile, in Fig. 2, it may still influence electrical device properties, for instance in a p^+n or a n^+p junction fabricated by ion implantation.

Summary

Ion implantations in a crystal target are commonly performed in non-channeling, "random", directions, but after a few nanometers, some ions will find low index channels, or planes, independent of the used impact angle where the stopping power is reduced. The impact angle can be used to modify the implanted ion distribution, but channeling cannot be avoided in crystalline 4H-SiC, only suppressed using non-channeling, "random", directions during implantation.

The energy loss is much lower for ions along some crystal directions. Hence, ion concentration versus depth profiles, will be broadened on the deep side for ion implantations in crystalline material compared amorphous targets. Using a 4° off angle, the main contribution in the deep tail is from ions following the $[000\bar{1}]$ direction, but some ions may follow crystal planes and other directions, like the $< 11\bar{2}\bar{3} >$ family. The contribution from planar channeling is closer to the surface while energy loss is smallest in the $< 11\bar{2}\bar{3} >$ channels and ions may travel to a substantial depth in these directions. At a depth of 1.2 μm in $< 11\bar{2}\bar{3} >$ some ions still retain more than 40% of the original kinetic energy.

Acknowledgment

References

[1] T. Kimoto, K. Kawahara, H. Niwa, N. Kaji and J. Suda, 2014 International Workshop on Junction Technology (IWJT), IEEE proceeings (2014) 1

[2] A. Hallén and M.K. Linnarsson, Surf. Coat. Tech. 306 (2016) 190.

[3] D.S. Gemmell, Rev. Mod. Phys. 46 (1974) 129.

[4] K. Nordlund, F. Djurabekova and G. Hobler, Phys. Rev. B94 (2016) 214109.

[5] A. Vantomme, Nucl. Instr. Meth. B371 (2016) 12.

[6] M.K. Linnarsson, A. Hallén and L. Vines, Semicond. Sci. Technol. 34 (2019) 115006.

[7] P. Pichler, T. Sledziewski, V. Häublein, A.J. Bauer and T. Erlbacher, Mater. Sc. Forum, 963, 386 (2019).

[8] M.K. Linnarsson, L. Vines, and A. Hallén, J. Appl. Phys. 130 (2021) 075701.

[9] K. Mochizuki, R. Kosugi, Y. Yonezawa and H. Okumura, Jpn. J. Appl. Phys 58 (2019) 050905.

[10] J. Wong-Leung, M.S. Janson and B.G. Svensson, J. Appl. Phys. 93 (2003) 8914.

[11] A. Hallén, M.K. Linnarsson and L. Vines, Mater. Sc. Forum, 963 (2019) 375.

[12] M.K. Linnarsson, A. Hallén, L. Vines and B.G. Svensson, Mater. Sc. Forum, 963 (2019) 382

[13] M.K. Linnarsson, A. Hallén, J. Åström, D. Primetzhofer, S. Legendre and G. Possnert, Rev. Sci. Instr. 83, 095107 (2012)

[14] M.S. Janson, PhD Thesis, KTH-Royal Institite of Technology, Department of Microelectronics and Information Technology, Materials and Semiconductor Physics Laboratory, Sweden, (2003) ISSN0284-0545.
http://www.diva-portal.org/smash/get/diva2:9286/FULLTEXT01.pdf
https://github.com/msjanson0.1/siimpl

[15] J.F. Ziegler, J.P. Biersack, and Y. Litmark, The stopping and ranges of ions in solids, Pergamon Press, 1985.

[16] J.P. Biersack and L. Haggmark, Nucl. Instr. Meth. 174 (1980) 257.

[17] M.S. Janson, M.K. Linnarsson, A. Hallén and B.G. Svensson, J. Appl. Phys. 96 (2004) 164.

[18] A. Zywietz, K. Karch and F. Bechstedt, Phys. Rev. B54 (1996) 1791.

[19] M.S. Janson, A. Hallén, P. Godignon, A.Yu. Kuzneetsov, M.K. Linnarsson, E. Morvan and B.G. Svensson, Mat. Sci. Forum 338-342 (2000) 889.

[20] See www.srim.org for "SRIM-2013".